Title

FLASH-RT does not affect chromosome translocations and junction structures beyond that of CONV-RT dose-rates.

Authors

Barghouth, Paul
Melemenidis, Stavros
Montay-Gruel, Pierre
et al.

Publication Date

2023-11-01

DOI

10.1016/j.radonc.2023.109906

Peer reviewed

HHS Public Access

Author manuscript

Radiother Oncol. Author manuscript; available in PMC 2024 November 01.

Published in final edited form as:

Radiother Oncol. 2023 November ; 188: 109906. doi:10.1016/j.radonc.2023.109906.

FLASH-RT does not affect chromosome translocations and junction structures beyond that of CONV-RT dose-rates

Paul G. Barghouth[a,#], **Stavros Melemenidis**[a], **Pierre Montay-Gruel**[b,c], **Jonathan Ollivier**[b], **Vignesh Viswanathan**[a], **Patrik G. Jorge**[d], **Luis A. Soto**[a], **Brianna C. Lau**[a], **Cheyenne Sadeghi**[a], **Anushka Edlabadkar**[a], **Richard Zhang**[c], **Ning Ru**[c], **Janet E. Baulch**[c], **Rakesh Manjappa**[a], **Jinghui Wang**[a], **Marie Le Bouteiller**[a], **Murat Surucu**[a], **Amy Yu**[a], **Karl Bush**[a], **Lawrie Skinner**[a], **Peter G. Maxim**[c], **Billy W. Loo Jr.**[a], **Charles L. Limoli**[c], **Marie-Catherine Vozenin**[b], **Richard L. Frock**[a,*]

[a]Department of Radiation Oncology, Stanford University School of Medicine, Stanford, CA 94305, USA

[b]Laboratory of Radiation Oncology, Department of Radiation Oncology. Lausanne University Hospital and University of Lausanne, Switzerland.

[c]Department of Radiation Oncology, University of California, Irvine, CA 92697-2695, USA.

[d]Institute of Radiation Physics/CHUV, Lausanne University Hospital, Switzerland.

Abstract

[*]Corresponding author: Richard L Frock; frock@stanford.edu.
[#]Present address: Nucleix, 10675 Sorrento Valley Road, Ste 250, San Diego, CA 92121

Author Contributions

PGB, CLL, M-CV, RLF designed the study. PGB, SM, PM-G, JO, VV, PGJ, RZ, NR, JEB performed experiments. PGB, CS, AE, MLB, RLF analyzed *HTGTS-JoinT-seq* data. SM, LAS, BCL performed and SM, RM, JW optimized Stanford dosimetry. PGJ, MS, AY, KB, LS, PGM, BWL Jr., CLL, M-CV supervised irradiations, machine, and dosimetry Q/A. RLF supervised the research. PGB and RLF wrote the manuscript. BWL Jr., CLL, and M-CV commented on and edited the manuscript.

CrediT author statement

Conceptualization: PGB, CLL, M-CV, RLF
Methodology: PGB, RLF
Software: PGB, MLB ,RM, JW, RLF
Validation: PGB, SM, LAS, BCL, PGJ, MS, AY, KB, LS, PGM, CLL, M-CV, RLF
Formal Analysis: PGB, SM, JO, CS, AE, RZ, MLB, RLF
Investigation: PGB, SM, PM-G, JO, VV, PGJ, RZ, NR, JEB
Resources: BWL Jr., CLL, M-CV, RLF
Data Curation: PGB, RLF
Writing – Original Draft: PGB, RLF
Writing – Review & Editing: BWL Jr., CLL, M-CV
Visualization: PGB, SM, JO, RZ, RLF
Supervision: BWL Jr., CLL, M-CV, RLF
Project Administration: BWL Jr., CLL, M-CV, RLF
Funding Acquisition: PGB, BWL Jr., CLL, M-CV, RLF

Competing Interest Statement

BWL Jr. has received research support outside this work from Varian Medical Systems, is a co-founder and board member of TibaRay, and is a consultant on a clinical trial steering committee for BeiGene. PGM is a co-founder of TibaRay. The other authors of this manuscript declare no conflict of interest.

Background and purpose: The impact of radiotherapy (RT) at ultra high vs conventional dose rate (FLASH vs CONV) on the generation and repair of DNA double strand breaks (DSBs) is an important question that remains to be investigated. Here, we tested the hypothesis as to whether FLASH-RT generates decreased chromosomal translocations compared to CONV-RT.

Materials and methods: We used two FLASH validated electron beams and high-throughput rejoin and genome-wide translocation sequencing (*HTGTS-JoinT-seq*), employing *S. aureus* and *S. pyogenes* Cas9 "bait" DNA double strand breaks (DSBs) in HEK239T cells, to measure differences in bait-proximal repair and their genome-wide translocations to "prey" DSBs generated after various irradiation doses, dose rates and oxygen tensions (normoxic, 21% O_2; physiological, 4% O_2; hypoxic, 2% and 0.5% O_2). Electron irradiation was delivered using a FLASH capable Varian Trilogy and the eRT6/Oriatron at CONV (0.08–0.13Gy/s) and FLASH (1×10^2-5×10^6 Gy/s) dose rates. Related experiments using clonogenic survival and γH2AX foci in the 293T and the U87 glioblastoma lines were also performed to discern FLASH-RT vs CONV-RT DSB effects.

Results: Normoxic and physioxic irradiation of HEK293T cells increased translocations at the cost of decreasing bait-proximal repair but were indistinguishable between CONV-RT and FLASH-RT. Although no apparent increase in chromosome translocations was observed with hypoxia-induced apoptosis, the combined decrease in oxygen tension with IR dose-rate modulation did not reveal significant differences in the level of translocations nor in their junction structures. Furthermore, RT dose rate modality on U87 cells did not change γH2AX foci numbers at 1- and 24-hours post-irradiation nor did this affect 293T clonogenic survival.

Conclusion: Irrespective of oxygen tension, FLASH-RT produces translocations and junction structures at levels and proportions that are indistinguishable from CONV-RT.

Keywords

HTGTS-JoinT-seq ; FLASH-RT; chromosome translocation; hypoxia; apoptosis

FLASH radiotherapy (RT) is an ultrafast irradiation modality, generally more than two orders of magnitude faster than conventional dose rate (CONV) RT, demonstrating a significant enhancement of normal tissue sparing while still maintaining effective tumor control in nearly all cases [1–4]. To this point, physical beam parameters may influence the magnitude, or the actual benefit provided by ultrahigh dose rate [5, 6]. Dose rate ≥40Gy/s is a putative threshold to achieve the "FLASH effect", which has been observed mostly *in vivo* across different tissues of small and large animals (reviewed in: [3, 4]). Early human clinical trials have also demonstrated feasibility of delivering FLASH dose rates [3, 7]. Despite the near consensus on the benefit of FLASH-RT over CONV-RT dose rates in experimental models, the mechanism explaining the FLASH effect remains to be elucidated.

A near instantaneous radioprotective hypoxic state afforded by FLASH-RT that could ultimately suppress DNA damage was proposed to explain the sparing effect of FLASH [8, 9]. In this context, DNA double strand break (DSB) measurements have largely been limited to measuring the kinetics of DNA damage response intermediates in cell lines and tissues [10, 11] or by measuring DNA strand breaks from supercoiled plasmids [12]. Therefore, to determine whether cell exposure to FLASH vs CONV dose rate imparts any changes to

DSB repair or pathway choice, a rigorous cellular genome-wide translocation assay that can measure DSBs from ionizing radiation (IR) is proposed in the present study.

High-Throughput Genome-wide Translocation Sequencing (*HTGTS*) [13] and its Linear Amplification Mediated (LAM) protocol [14, 15], leverages the generation of a fixed "bait" DSB to capture "prey" DSBs via their chromosome translocation to each other and maps the resulting prey end of the junction (or joint) at single nucleotide resolution. *LAM-HTGTS* has been used extensively to quantify translocations generated from designer endonucleases [14, 16–18], physiologic DSBs [19–22] and IR [14]. ReJoin and Translocation sequencing (*JoinT-seq*) built upon the *LAM-HTGTS* platform by additionally quantifying proximal repair outcomes (e.g. deletions) of the bait "Breaksite" along with genome-wide translocations and recently described DSB repair in the context of core nonhomologous end joining (NHEJ) deficiency of G1-arrested cells [22]. Here, *HTGTS-JoinT-seq* is employed to identify alterations in translocations and/or proximal repair affected by two different FLASH-RT validated electron beams [23] under varied oxygen tensions in 293T cells, a human embryonic kidney cell line transformed by the E1 gene of human adenovirus 5 and the SV40 large T antigen [24] used as a tool to perform HTGTS. Interestingly and although enrichment of translocations is dose-dependent and is separately attenuated by hypoxic oxygen tensions, FLASH-RT does not confer any significant decrease in translocations or alteration of junction structures beyond that imposed by CONV-RT, suggesting that both modalities of dose delivery induce similar DDR in this *in vitro* model.

Materials and Methods

Cell culture and Cas9 plasmids.

HEK293T and U87 cell lines were cultured at 37°C, 5% CO_2 using DMEM supplemented with glutamine, 10% FCS and 0.5% penicillin/streptomycin. The following *S. aureus* Cas9 plasmids were kindly provided by Manuel Gonçalves (Leiden): BA15_pCAG.SaCas9.rBGpA (SaCas9 nuclease) and AV85_pSa-gRAG1.1 (encoding RAG1-specific Sa-gRNA1.1) [16, 18]. *S pyogenes* Cas9 plasmid, pX330-U6-Chimeric_BB-CBh-hSpCas9, was obtained from Addgene (#42230). RAG1B gRNA cloning and pCMX-eGFP have been previously described [14]. See supplement for more details.

Oxygen tension.

SaCas9:RAG1.1-transfected cells were either kept at room air (21% O_2) set to 37°C or placed into a controlled atmosphere chamber (InVivo2 Hypoxic Workstation at Stanford and Biospherix hypoxia hood at CHUV) at physiologic or hypoxic oxygen tensions of 4%, 2%, or 0.5% O_2 set to 37°C. A portable hypoxic chamber OxyGenie (Baker) was used to transport cells to and from the radiation facility at Stanford. See supplement for more details.

Irradiation Exposure.

SaCas9:RAG1.1 experiments and U87 cell line irradiations were performed at Stanford University using a Varian Trilogy medical LINAC (Varian Medical Systems, Inc., Palo Alto, CA) configured for ultra-high dose rate electron beam delivery. SpCas9:RAG1B

experiments and clonogenic survival were performed at CHUV Lausanne University Hospital using Oriatron eRT6 electron beam LINAC (PMB Alcen). See supplement for beam parameters.

Flow cytometry analysis.

Cells were measured for GFP (transfection) and 7AAD (BD) (cell death) at end points for *HTGTS-JoinT-seq* or for PI/FITC-Annexin V (Biolegend) staining for apoptosis detection. In all cases, untransfected cells were subjected to no, single, and double staining to optimize gating.

HTGTS-JoinT-seq.

12μg input DNA complexity was used to enrich for junction libraries; primers for SaCas9:RAG1.1 [16, 18] and SpCas9:RAG1B [14, 17] bait DSBs were previously described. SpCas9:RAG1B libraries were sequenced using MiSeq (250PE) and normalized to 214,700 sequence reads. SaCas9:RAG1.1 libraries were sequenced by NovaSeq (150PE) and normalized to 904,846 sequence reads. Sequence data were processed as described [22] and aligned to hg38 genome build. MACS2 identified hotspots as described [14].

Statistics.

Graphs were generated by Prism 9. Where indicated in figure legends, tests for statistical significance were evaluated for all values in each graph using either t-test or ANOVA with posttest for significance of multiple comparisons using the associated Prism 9 software.

Results

We first assayed proximal and genome-wide DSB repair outcomes influenced only by CONV-RT. For all experiments described, we distinguished translocations versus bait-proximal repair (termed as the “Breaksite”) by separating recovered prey junctions aligned outside versus inside, respectively, a 500kb window flanking each side of the bait DSB since spreading of the phosphorylated H2AX (γH2AX) damage signal covers a range of hundreds of kilobases up to several megabases [25–27]. We employed the *S. aureus* Cas9 bait DSB targeting the RAG1 locus on chromosome 11 using the RAG1.1 guide RNA (SaCas9:RAG1.1) in 293T cells [16, 18], which has a higher substrate turnover rate in comparison to the commonly used *S. pyogenes* Cas9 [28], and assayed for repair outcome differences over a 24 hour period after 10 Gy exposure from a CONV-RT electron beam clinical linear accelerator (LINAC; Stanford) [29, 30] (Fig. 1A). Cell death was minimally increased with irradiation, and the cell fractions with transfected GFP reporter/Cas9 plasmids were relatively high by flow cytometry (Fig. 1B) prior to collection for *JoinT-seq* library preparation and sequencing.

Approximately half a million total junctions were recovered for the non-irradiated (No IR) control (Table S1); two previously identified RAG1.1 off-target hotspots on chromosomes 1 and 8 [16, 18] were identified again (Fig. 1C). Deeper analysis revealed ~94% of junctions aligned within the bait Breaksite (Fig. 1C, D; Table S1), with most of the total (~90%) generating small (≤25bp) deletions as a direct result of rejoining bait DSB ends

(Fig. S1A, B) [22]. Beyond the Breaksite window, intrachromosomal translocations were ~150-fold less frequent; however, interchromosomal translocations were ~8-fold greater than their intrachromosomal counterpart, averaging ~9,100 junctions (Fig. 1E; Table S1). Both translocation subgroups predominantly harbored direct, with some short microhomology (MH), joints, consistent with NHEJ utilization (Fig. 1F) [31]; although, translocations significantly relied more on long MHs in contrast to small deletions (~3% vs. ~13%)(Fig. S1C).

CONV-RT resulted in a total net loss in recovered junctions by 12% and specifically affected bait Breaksite junctions (Fig. 1C, D; Fig. S1B; Table S1). Correspondingly, CONV-RT increased genome-wide translocations 2.1-fold, totaling ~69,000 translocations (~22,900 on average) (Fig. 1C, E; Table S1). Crucially, intrachromosomal translocations outgained interchromosomal translocations by nearly 4-fold, rendering the chromosome harboring the bait DSB a hotspot for translocation (Fig. 1C, E; Table S1). Despite the increased genome-wide translocations, CONV-RT did not alter their junction structure proportions (Fig. S1D), suggesting the bulk of translocations from both spontaneous DSBs and IR-generated DSBs are repaired in a similar manner. Thus, we conclude CONV-RT from electron beam LINAC (Table S2) imparts a similar translocation enrichment pattern as previously observed using X-Ray sources [14, 32].

We next sought to describe genome-wide translocations in the context of varied oxygen tensions. Culture of 293T cells at hypoxic oxygen tensions (2% & 0.5% O_2) over 24 hours did not reveal a dramatic change in cell death (<10%) relative to the normoxic (21% O_2; air) environment. However, cell death was significantly increased over a 48-hour period, particularly for 0.5% O_2 oxygen tensions, affecting 45–75% of the population (Fig. S2A), suggesting potentially increased levels of translocations. SaCas9:Rag1.1 was transiently delivered into 293T cells and split into three oxygen tensions–21% O_2, 2% O_2, and 0.5% O_2—and assayed for repair after 48 hours (Fig. 2A). Transfection was efficient in all three conditions despite reproducing an O_2 level-dependent effect on cell death (Fig. S2B). Total recovered junctions for normoxic cells were nearly 600,000 but were progressively decreased by 15–25% as oxygen tension attenuated (Fig. 2B; Table S1). In striking contrast to CONV-RT (see Fig. 1), junctions from both translocations and the bait Breaksite were decreased 10–25% under hypoxic conditions (Fig. 2C, D; Table S1). Hypoxia did not affect translocation junction structure distributions (Fig. S2C) but small deletions in the Breaksite used progressively less (3–5%) polymerase-mediated insertions (Fig. S2D). Despite the high level of cell death from chronic hypoxia, we could not identify any discernible increase in chromosome translocations. We revisited the type of cell death occurring at 48 hours of hypoxia and found most of the dying cells were apoptotic (Fig. S2E, F). To confirm whether cycling cells were specifically impacted by hypoxia as concluded from earlier studies [33], we measured for apoptosis in cycling and G1-arrested Abelson kinase-transformed progenitor B cells [22] with decreasing O_2 levels over 48 hours and found cycling cells, but not the G1-arrested population, were subjected to increasing apoptosis as a function of decreasing O_2 (Fig. S2F). Thus, we conclude chronic pathologic hypoxia induces apoptosis in cycling cells but curiously does not increase the level of translocations.

To discern FLASH dose-rate effects on DSB repair, we first assayed repair at physioxic oxygen tension (4% O_2) employing the more commonly used *S. pyogenes* Cas9 (SpCas9), and gRNA bait, RAG1B [14] targeting a DSB 45bp away from the SaCas9:RAG1.1 DSB site. Here, transfected 293T cells (Fig. S3A) were transitioned to 4% O_2 environment and irradiated with 10 Gy using either an X-Ray tube (0.06Gy/s) or an eRT6 electron beam LINAC set for CONV-RT (0.21Gy/s) or FLASH-RT (1,000Gy/s) (CHUV) (Fig. 3A; Table S2). Recovered junctions for the control totaled just over 70,000 and RAG1B off-target DSB hotspots were again found on chromosomes 14 and 4 (Fig. 3A; Table S1), as previously reported [14, 17]. Analogous to the SaCas9:RAG1.1 bait, the SpCas9:RAG1B bait Breaksite consisted of ~90% of total junctions followed by interchromosomal and intrachromosomal translocations (Fig. 3A–C; Table S1). Similarly, all irradiated samples resulted in fewer junctions recovered (25–33% less than control), with a 2-fold decrease in bait Breaksite repair and a characteristic increase of intrachromosomal translocations that, combined with interchromosomal translocation gains, led to a ~6-fold increase in total translocations (Fig. 3A–C; Table S1). Crucially, we did not observe any significant differences in translocation numbers or junction structures between radiation sources or dose-rate modalities at 4% O_2 (Fig. 3C–D; Table S1), and clonogenic survival did not reveal any significant difference between CONV-RT and FLASH-RT (Fig. S3B; Table S3). We conclude IR dose rate modulation does not impact translocations and cell survival for 293T cells at physioxic oxygen tension. In support of this conclusion, additional CONV-RT and FLASH-RT experiments (Stanford) using the U87 glioblastoma cell line and measuring DSBs by γH2AX foci counts at 1 and 24 hours post-irradation did not reveal differences between IR dose rate modality in foci numbers (Fig. S4).

Finally, we sought to identify any potential translocation differences between CONV-RT and FLASH-RT at pathologic hypoxic oxygen tension (0.5% O_2), where the FLASH effect may be most pronounced. SaCas9:RAG1.1 transfected 293T cells cultured in normoxic or hypoxic conditions, transported either in tubes or in a portable environment-controlled apparatus (i.e., OxyGenie), and irradiated under CONV-RT or FLASH-RT settings (Stanford) (Figs. 4A; S5A–C)(see methods and supplement). Gafchromic film dosimetry confirmed CONV and FLASH dose-rates delivered per replication (Fig. 4B; Table S2). For all conditions assayed (oxygen tension and dose-rate; 4 irradiation doses and 1 non-irradiated control for each combination), transfection efficiency was consistently high and cell death for hypoxic cultures ranged 30–50% (Fig. S5D). Total recovered junctions across normoxic controls ranged between ~452,000–677,000 with hypoxia decreasing recovered junctions by 5–12% (Figs. S6A, S7A; Table S1); overall, irradiation depressed total recovered junctions (Figs. S6A–C; S7A–C; Table S1). As predicted, the fraction of translocations was progressively increased as a function of IR dose (Figs. 4C, D; S6A–C; S7A–C; Table S1). In this regard, irradiation under pathologic hypoxia also yielded increased translocations, though the rate increase with absorbed dose increase was shallower (Fig. 4C, D; Table S1). Hypoxia together with irradiation did not alter translocation junction structure distributions (Fig. S5E). Importantly, translocation numbers and junction structures between CONV-RT and FLASH-RT at comparable absorbed doses and oxygen tensions were indistinguishable (Fig. 4C, D; S5E; Table S1). We conclude that irradiation dose rate at pathologic hypoxic oxygen tensions does not affect translocation formation and frequency.

Discussion

The goal of this study was to determine whether any molecular differences in DSB repair or translocations could be identified after HEK293T cell exposure to various doses, dose rates and oxygen tensions. The premise was that potential molecular alterations in DSB repair outcomes afforded by FLASH dose rates might differ from those occurring at conventional dose rate. The HEK293T line, which is not tumor-derived but was transformed by multiple agents *in vitro* [24], was used postulating that alterations to the formation of DSBs and translocation would be discerned irrespective of normal or transformed status. To date, the classical *in vitro* and *in vivo* methods used to study DNA damage and repair have failed to produce evidence that ultra-high dose rate could dramatically modify these processes. For years the field has realized that radiation chemistry tracks linearly with dose, but that the response of different biological systems to radiolytic damage provides variability in radiation sensitivity that depends on total dose, radiation quality, antioxidant levels and repair capacity (among other factors). Multiple and distinctly different normal tissues have routinely exhibited FLASH sparing of normal tissue toxicity, while multiple and distinctly different tumor types grown in select mouse models have routinely exhibited similar tumorigenic responses to FLASH and CONV irradiation. Available DNA damage and repair data have largely focused on measuring differences in the appearance and disappearance of DNA repair foci (γH2AX and 53BP1) between normal and cancer cells [10, 11, 29]. While relatively minor differences in dose rate dependent residual damage levels normalize past 24h, repair outcome has never been investigated properly. Thus, we decided to implement a unique and validated cellular system for quantifying translocation frequencies and junction structure to evaluate possible differences between FLASH and CONV irradiation.

Using *HTGTS-JoinT-seq* [22], we found IR dose-rate to have no significant impact on translocations and proximal repair beyond the intended absorbed dose, across a wide range of oxygen tensions, and as determined using two different FLASH irradiators. While these data do not formally rule out potential dose-rate dependent differences in the yields of other radiolytic lesions (single strand breaks, base damage), present results clearly indicate that the induction and repair of DSB lesions is not dose-rate dependent with regard to the cells and range of dose rate assayed here. Furthermore, based on these and other available data [4], the potential role of DNA damage and repair as an underlying mechanism of the FLASH effect seems implausible.

We also discovered oxygen tensions down to 0.5% O_2 did not induce substantial apoptosis in 293T cells until after 24 hours of low oxygen tensions. Here, the replicating cell cycle phases (S-G2/M) are implicated in the cell death phenotype since G1-arrest did not significantly increase apoptosis detection. The cell death mechanism and response observed under chronic hypoxia is similar to what has been previously described in 24-hour cultures, but under extremely low oxygen tension (<0.1% O_2), resulting initially in a stressed, but sustained, replication from a limiting nucleotide pool with eventual stalling and, ultimately, replisome unloading beyond 12 hours of extreme hypoxia [33–35]. In this context, hypoxia-mediated activation of the DNA damage kinases and phosphorylation of H2AX [33, 36, 37] are necessary to stabilize stalled replication forks and to suppress apoptosis. Yet, despite

a high level of apoptosis observed at 48 hours of low oxygen tensions in our studies, additional translocations were not detected.

The above findings agree with early-stage apoptosis observations demonstrating pan-nuclear or nuclear-peripheral γH2AX staining that are not enriched with DSB repair markers, unlike with individual DNA damage foci [38, 39] or micronuclei [40, 41]. However, further insight comes from a recent study that determined apoptotic DNA fragmentation generates extrachromosomal circular DNA elements (eccDNAs) with singular DNA alignments and size distributions varying in units of nucleosome occupancy [42]. In this regard, genome-wide circularization of DNA fragments, resulting in the formation of potent immunostimulants for dendritic cells and macrophages, requires DNA ligase III, but not the NHEJ ligase, DNA ligase IV [42]. Therefore, hypoxia-induced apoptotic eccDNA precursors would not be translocation substrates for Cas9 bait DSBs in human cells [31]. We speculate repair pathway incompatibility along with other contributing factors—(1) frequency and proximity of eccDNA precursor ends to each other relative to the bait DSB, (2) end accessibility differences, and (3) caspase-mediated cleavage of repair proteins [14, 16, 22, 43, 44]—are at play to promote the cell death program and to stimulate phagocytosis of apoptotic bodies. A deeper investigation into apoptotic DNA recombination will be necessary to better understand mechanisms driving eccDNA biogenesis and any potential role eccDNAs have in explaining the FLASH effect *in vivo*.

Supplementary Material

Refer to Web version on PubMed Central for supplementary material.

Acknowledgements

The authors thank Manuel Gonçalves (LUMC) for providing the SaCas9:Rag1.1 vectors, Erinn Rankin lab and Baker Ruskinn for the OxyGenie device, and members of the BWL Jr, CLL, M-CV, and RLF labs for discussion and feedback. This work was supported by the NIH Ruth L. Kirschstein National Research Service Award fellowship T32CA121940 (to PGB), the Radiation Research Foundation Career Development Award (to RLF) and by the NCI grant P01CA244091 (to BWL Jr., M-CV and CLL). RLF was a V Scholar for the V Foundation for Cancer Research (V2019–003) and is an American Cancer Society Research Scholar (RSG-23-1038994-01-DMC). We also gratefully acknowledge philanthropic donors to the Department of Radiation Oncology at Stanford.

Data Availability

Illumina sequencing data are available through GEO (GSE227466).

References

[1]. Favaudon V, Caplier L, Monceau V, Pouzoulet F, Sayarath M, Fouillade C, et al. Ultrahigh dose-rate FLASH irradiation increases the differential response between normal and tumor tissue in mice. Sci Transl Med 2014;6:245ra93.

[2]. Kacem H, Almeida A, Cherbuin N, Vozenin MC. Understanding the FLASH effect to unravel the potential of ultra-high dose rate irradiation. Int J Radiat Biol 2022;98:506–16. [PubMed: 34788193]

[3]. Vozenin MC, Bourhis J, Durante M. Towards clinical translation of FLASH radiotherapy. Nat Rev Clin Oncol 2022;19:791–803. [PubMed: 36303024]

[4]. Limoli CL, Vozenin MC. Reinventing Radiobiology in the Light of FLASH Radiotherapy. Annual Review of Cancer Biology 2023;7:1–21.

[5]. Schuler E, Acharya M, Montay-Gruel P, Loo BW Jr, Vozenin MC, Maxim PG Ultra-high dose rate electron beams and the FLASH effect: From preclinical evidence to a new radiotherapy paradigm. Med Phys 2022;49:2082–95. [PubMed: 34997969]

[6]. Wilson JD, Hammond EM, Higgins GS, Petersson K. Corrigendum: Ultra-High Dose Rate (FLASH) Radiotherapy: Silver Bullet or Fool's Gold? Front Oncol 2020;10:210. [PubMed: 32161721]

[7]. Bourhis J, Sozzi WJ, Jorge PG, Gaide O, Bailat C, Duclos F, et al. Treatment of a first patient with FLASH-radiotherapy. Radiother Oncol 2019;139:18–22. [PubMed: 31303340]

[8]. Pratx G, Kapp DS. Ultra-High-Dose-Rate FLASH Irradiation May Spare Hypoxic Stem Cell Niches in Normal Tissues. Int J Radiat Oncol Biol Phys 2019;105:190–2. [PubMed: 31145965]

[9]. Spitz DR, Buettner GR, Petronek MS, St-Aubin JJ, Flynn RT, Waldron TJ, et al. An integrated physico-chemical approach for explaining the differential impact of FLASH versus conventional dose rate irradiation on cancer and normal tissue responses. Radiother Oncol 2019;139:23–7. [PubMed: 31010709]

[10]. Fouillade C, Curras-Alonso S, Giuranno L, Quelennec E, Heinrich S, Bonnet-Boissinot S, et al. FLASH Irradiation Spares Lung Progenitor Cells and Limits the Incidence of Radio-induced Senescence. Clin Cancer Res 2020;26:1497–506. [PubMed: 31796518]

[11]. Levy K, Natarajan S, Wang J, Chow S, Eggold JT, Loo PE, et al. Abdominal FLASH irradiation reduces radiation-induced gastrointestinal toxicity for the treatment of ovarian cancer in mice. Sci Rep 2020;10:21600. [PubMed: 33303827]

[12]. Perstin A, Poirier Y, Sawant A, Tambasco M. Quantifying the DNA-damaging Effects of FLASH Irradiation With Plasmid DNA. Int J Radiat Oncol Biol Phys 2022;113:437–47. [PubMed: 35124135]

[13]. Chiarle R, Zhang Y, Frock RL, Lewis SM, Molinie B, Ho YJ, et al. Genome-wide translocation sequencing reveals mechanisms of chromosome breaks and rearrangements in B cells. Cell 2011;147:107–19. [PubMed: 21962511]

[14]. Frock RL, Hu J, Meyers RM, Ho YJ, Kii E, Alt FW. Genome-wide detection of DNA double-stranded breaks induced by engineered nucleases. Nat Biotechnol 2015;33:179–86. [PubMed: 25503383]

[15]. Hu J, Meyers RM, Dong J, Panchakshari RA, Alt FW, Frock RL. Detecting DNA double-stranded breaks in mammalian genomes by linear amplification-mediated high-throughput genome-wide translocation sequencing. Nat Protoc 2016;11:853–71. [PubMed: 27031497]

[16]. Chen X, Tasca F, Wang Q, Liu J, Janssen JM, Brescia MD, et al. Expanding the editable genome and CRISPR-Cas9 versatility using DNA cutting-free gene targeting based on in trans paired nicking. Nucleic Acids Res 2020;48:974–95. [PubMed: 31799604]

[17]. Paulsen BS, Mandal PK, Frock RL, Boyraz B, Yadav R, Upadhyayula S, et al. Ectopic expression of RAD52 and dn53BP1 improves homology-directed repair during CRISPR-Cas9 genome editing. Nat Biomed Eng 2017;1:878–88. [PubMed: 31015609]

[18]. Wang Q, Liu J, Janssen JM, Le Bouteiller M, Frock RL, Goncalves M. Precise and broad scope genome editing based on high-specificity Cas9 nickases. Nucleic Acids Res 2021;49:1173–98. [PubMed: 33398349]

[19]. Lattanzi A, Camarena J, Lahiri P, Segal H, Srifa W, Vakulskas CA, et al. Development of beta-globin gene correction in human hematopoietic stem cells as a potential durable treatment for sickle cell disease. Sci Transl Med 2021;13.

[20]. Willis NA, Frock RL, Menghi F, Duffey EE, Panday A, Camacho V, et al. Mechanism of tandem duplication formation in BRCA1-mutant cells. Nature 2017;551:590–5. [PubMed: 29168504]

[21]. Zhao L, Frock RL, Du Z, Hu J, Chen L, Krangel MS, et al. Orientation-specific RAG activity in chromosomal loop domains contributes to Tcrd V(D)J recombination during T cell development. J Exp Med 2016;213:1921–36. [PubMed: 27526713]

[22]. Liang Z, Kumar V, Le Bouteiller M, Zurita J, Kenrick J, Lin SG, et al. Ku70 suppresses alternative end joining in G1-arrested progenitor B cells. Proc Natl Acad Sci U S A 2021;118:e2103630118. [PubMed: 34006647]

[23]. Jorge PG, Melemenidis S, Grilj V, Buchillier T, Manjappa R, Viswanathan V, et al. Design and validation of a dosimetric comparison scheme tailored for ultra-high dose-rate electron beams

to support multicenter FLASH preclinical studies. Radiother Oncol 2022;175:203–9. [PubMed: 36030934]

[24]. Reus JB, Trivino-Soto GS, Wu LI, Kokott K, Lim ES. SV40 Large T Antigen Is Not Responsible for the Loss of STING in 293T Cells but Can Inhibit cGAS-STING Interferon Induction. Viruses 2020;12. [PubMed: 33374816]

[25]. Arnould C, Rocher V, Finoux AL, Clouaire T, Li K, Zhou F, et al. Loop extrusion as a mechanism for formation of DNA damage repair foci. Nature 2021;590:660–5. [PubMed: 33597753]

[26]. Rogakou EP, Pilch DR, Orr AH, Ivanova VS, Bonner WM. DNA double-stranded breaks induce histone H2AX phosphorylation on serine 139. J Biol Chem 1998;273:5858–68. [PubMed: 9488723]

[27]. Yin B, Savic V, Juntilla MM, Bredemeyer AL, Yang-Iott KS, Helmink BA, et al. Histone H2AX stabilizes broken DNA strands to suppress chromosome breaks and translocations during V(D)J recombination. J Exp Med 2009;206:2625–39. [PubMed: 19887394]

[28]. Yourik P, Fuchs RT, Mabuchi M, Curcuru JL, Robb GB. Staphylococcus aureus Cas9 is a multiple-turnover enzyme. RNA 2019;25:35–44. [PubMed: 30348755]

[29]. Kim YE, Gwak SH, Hong BJ, Oh JM, Choi HS, Kim MS, et al. Effects of Ultra-high doserate FLASH Irradiation on the Tumor Microenvironment in Lewis Lung Carcinoma: Role of Myosin Light Chain. Int J Radiat Oncol Biol Phys 2021;109:1440–53. [PubMed: 33186615]

[30]. Schuler E, Trovati S, King G, Lartey F, Rafat M, Villegas M, et al. Experimental Platform for Ultrahigh Dose Rate FLASH Irradiation of Small Animals Using a Clinical Linear Accelerator. Int J Radiat Oncol Biol Phys 2017;97:195–203. [PubMed: 27816362]

[31]. Ghezraoui H, Piganeau M, Renouf B, Renaud JB, Sallmyr A, Ruis B, et al. Chromosomal translocations in human cells are generated by canonical nonhomologous end-joining. Mol Cell 2014;55:829–42. [PubMed: 25201414]

[32]. Zhang Y, McCord RP, Ho YJ, Lajoie BR, Hildebrand DG, Simon AC, et al. Spatial organization of the mouse genome and its role in recurrent chromosomal translocations. Cell 2012;148:908–21. [PubMed: 22341456]

[33]. Hammond EM, Denko NC, Dorie MJ, Abraham RT, Giaccia AJ. Hypoxia links ATR and p53 through replication arrest. Mol Cell Biol 2002;22:1834–43. [PubMed: 11865061]

[34]. Foskolou IP, Jorgensen C, Leszczynska KB, Olcina MM, Tarhonskaya H, Haisma B, et al. Ribonucleotide Reductase Requires Subunit Switching in Hypoxia to Maintain DNA Replication. Mol Cell 2017;66:206–20 e9. [PubMed: 28416140]

[35]. Olcina MM, Foskolou IP, Anbalagan S, Senra JM, Pires IM, Jiang Y, et al. Replication stress and chromatin context link ATM activation to a role in DNA replication. Mol Cell 2013;52:758–66. [PubMed: 24268576]

[36]. Bencokova Z, Kaufmann MR, Pires IM, Lecane PS, Giaccia AJ, Hammond EM. ATM activation and signaling under hypoxic conditions. Mol Cell Biol 2009;29:526–37. [PubMed: 18981219]

[37]. Myers K, Gagou ME, Zuazua-Villar P, Rodriguez R, Meuth M. ATR and Chk1 suppress a caspase-3-dependent apoptotic response following DNA replication stress. PLoS Genet 2009;5:e1000324. [PubMed: 19119425]

[38]. Marti TM, Hefner E, Feeney L, Natale V, Cleaver JE. H2AX phosphorylation within the G1 phase after UV irradiation depends on nucleotide excision repair and not DNA double-strand breaks. Proc Natl Acad Sci U S A 2006;103:9891–6. [PubMed: 16788066]

[39]. Solier S, Pommier Y. The nuclear gamma-H2AX apoptotic ring: implications for cancers and autoimmune diseases. Cell Mol Life Sci 2014;71:2289–97. [PubMed: 24448903]

[40]. Crasta K, Ganem NJ, Dagher R, Lantermann AB, Ivanova EV, Pan Y, et al. DNA breaks and chromosome pulverization from errors in mitosis. Nature 2012;482:53–8. [PubMed: 22258507]

[41]. Ly P, Teitz LS, Kim DH, Shoshani O, Skaletsky H, Fachinetti D, et al. Selective Y centromere inactivation triggers chromosome shattering in micronuclei and repair by non-homologous end joining. Nat Cell Biol 2017;19:68–75. [PubMed: 27918550]

[42]. Wang Y, Wang M, Djekidel MN, Chen H, Liu D, Alt FW, et al. eccDNAs are apoptotic products with high innate immunostimulatory activity. Nature 2021;599:308–14. [PubMed: 34671165]

[43]. Frock RL, Sadeghi C, Meng J, Wang JL. DNA End Joining: G0-ing to the Core. Biomolecules 2021;11:1487. [PubMed: 34680120]

[44]. Julien O, Wells JA. Caspases and their substrates. Cell Death Differ 2017;24:1380–9. [PubMed: 28498362]

Highlights:

- Radiotherapy enhances frequency of genome-wide translocations.
- Hypoxia-induced apoptotic DNA intermediates are not translocation substrates.
- IR dose-rate variance does not alter translocation junction structures.
- Oxygen tension does not affect translocations formed between FLASH vs. CONV.

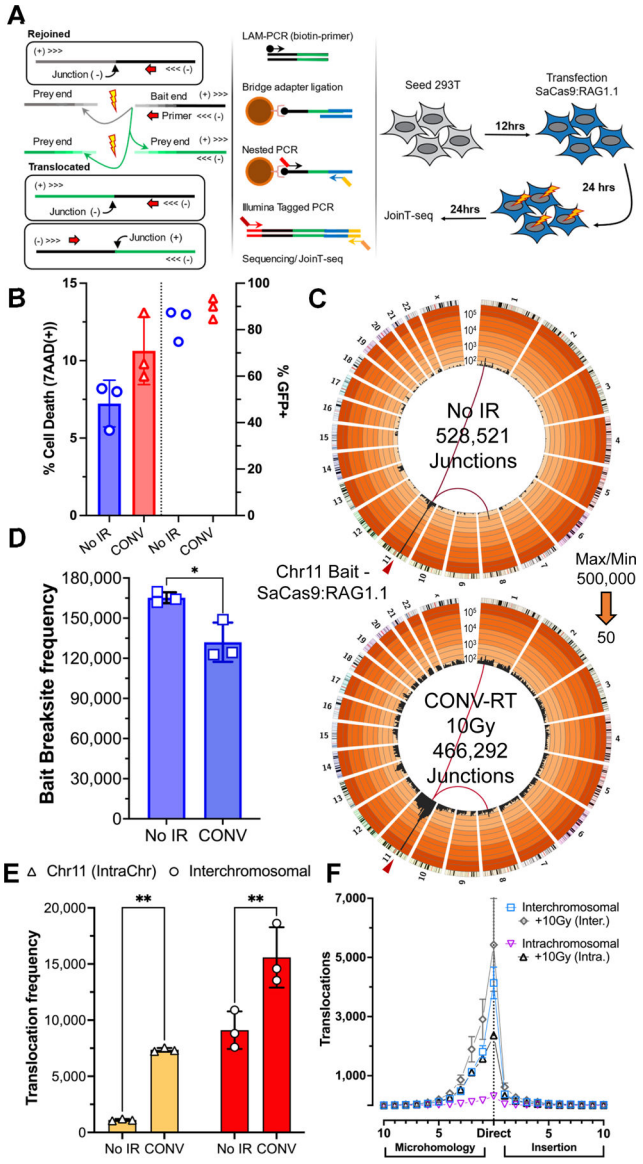

Fig. 1. Intrachromosomal translocations are dramatically increased after CONV-RT.

(A) Strategy for *HTGTS-JoinT-seq*, SaCas9:gRNA delivery, electron beam irradiation and collection for *JoinT-seq* analysis. (B) Cell death and transfection efficiency measures by flow cytometry. (C) Circos plots describing translocations in 5Mb binned regions across each chromosome (black bars) displayed on a custom 1,2,5 iteration log scale with increasingly darker orange coloring indicating greater orders of magnitude scaling; Max/Min ranges are indicated. Red triangle indicates position of the bait DSB bin and inclusive of the bait Breaksite window (N=3 each). (D) Junction frequencies within the bait Breaksite; unpaired t-test: *P < 0.05. (E) Intra- and interchromosomal translocation frequencies; two-way ANOVA with Šidák posttest: **P < 0.01. (F) Translocation junction structure distributions.

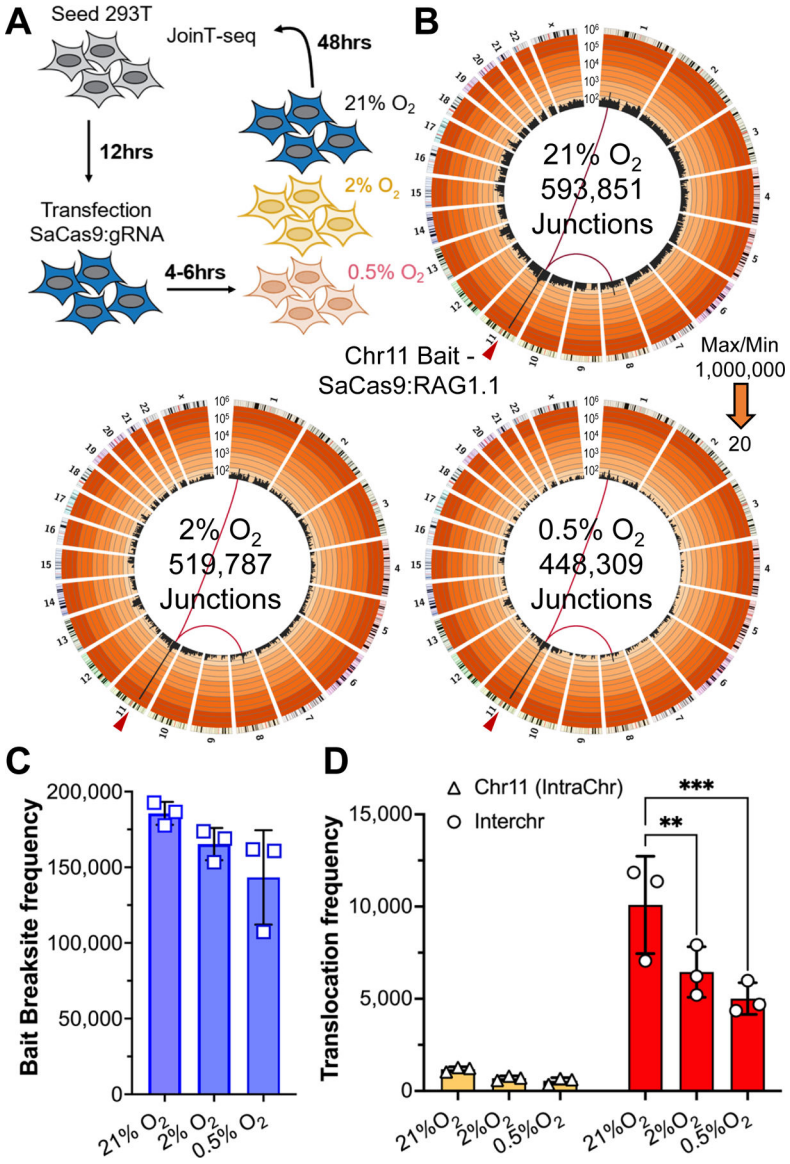

Fig. 2. Chronic hypoxia does not induce translocations.

(A) Strategy to detect translocations under different oxygen tensions. (B) Circos plots as described in Figure 1 (N=3 each). Max/Min range is indicated. (C) Bait Breaksite frequencies; one-way ANOVA with Dunnett's posttest: no significance below $P < 0.05$. (D) Translocation frequencies; two-way ANOVA with Dunnett's posttest: **$P < 0.01$, ***$P < 0.001$.

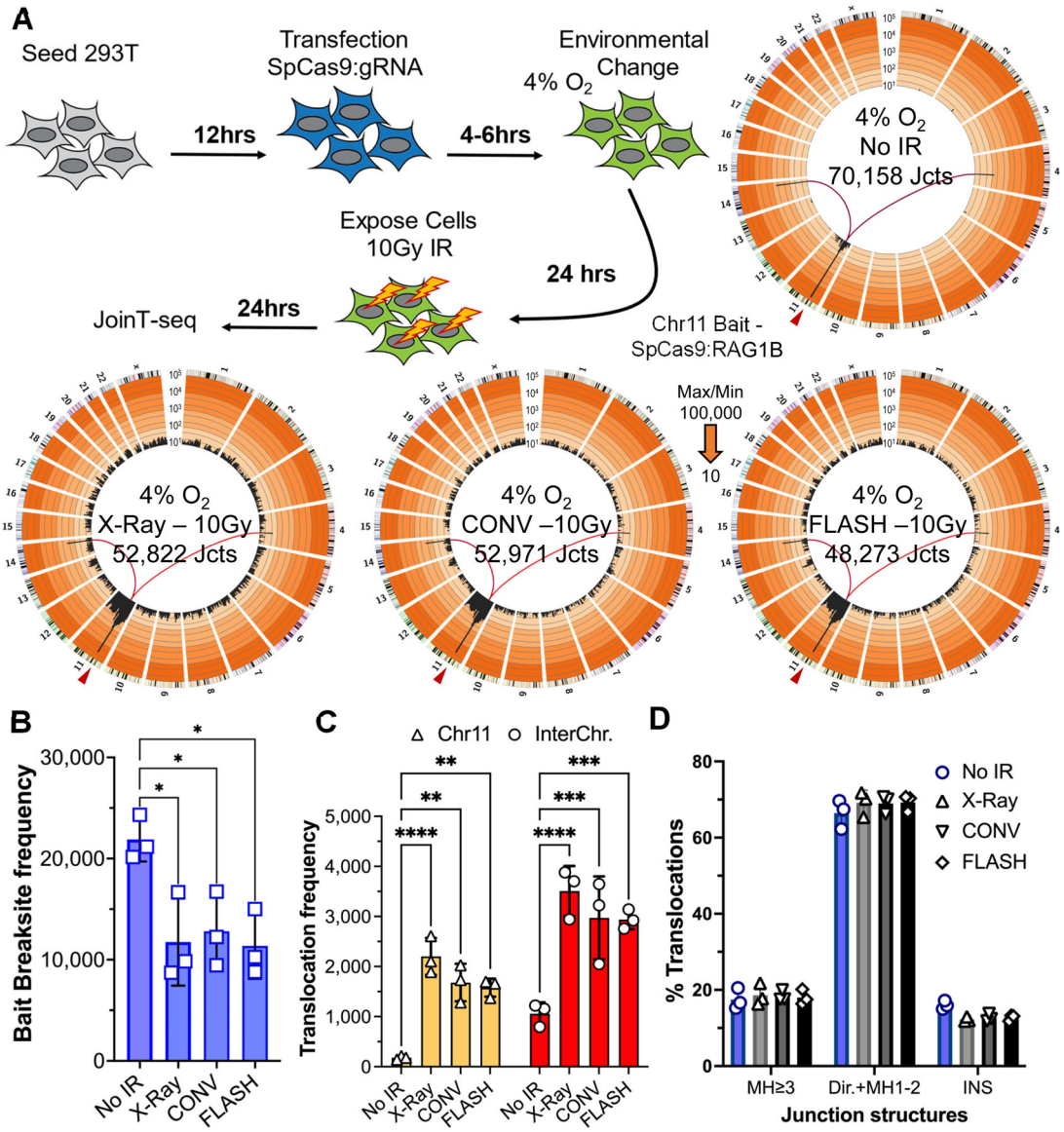

Fig. 3. Translocations remain undifferentiated between dose rates at 4% O_2.

(A) Physioxic irradiation strategy and resulting circos plots from control, X-Ray, CONV, and FLASH irradiated samples (N=3 each). (B) Bait-proximal junction frequencies; One-way ANOVA with Dunnett's posttest: *P < 0.05. (C) Translocation frequencies; **P < 0.01, ***P < 0.001, ****P < 0.0001. (D) Translocation junction structure distributions split into three groups: long microhomologies (MH≥3), direct with short MHs (Dir+MH1−2), and insertions (INS); two-way ANOVA with Tukey posttest: no significance below P < 0.05.

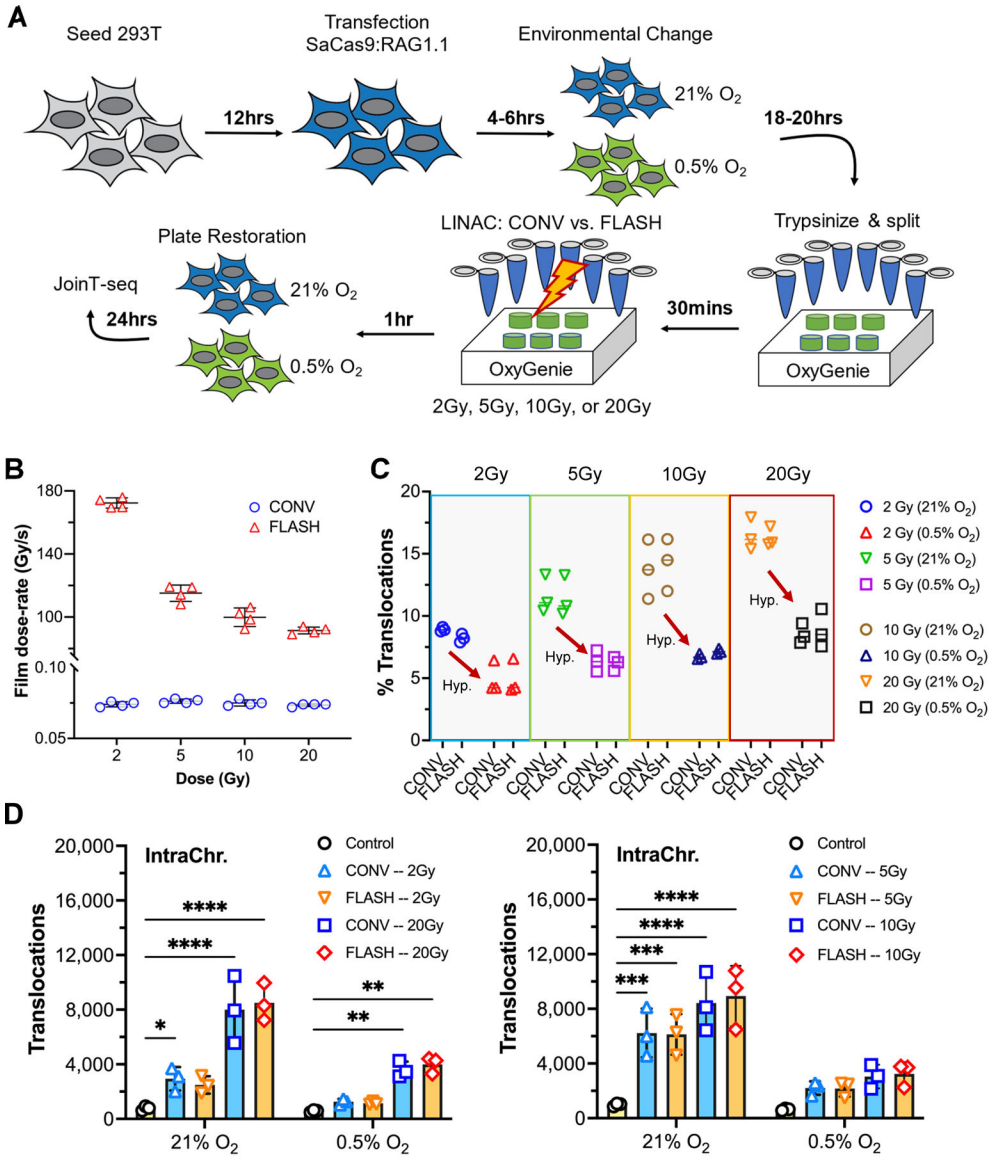

Fig. 4. FLASH-RT and CONV-RT display similar translocation increases with increasing dose.

(A) Strategy for normoxic and hypoxic irradiation measures for JoinT-seq. Cells in both environments were trypsinized and maintained in their respective oxygen tensions during irradiation. (B) Film dose rates plotted for each experiment (N=3) (C) Percent of translocations for each dose rate/environment/absorbed dose over a 2 Gy–20 Gy range. (D) Intrachromosomal translocation frequency gains with increasing absorbed IR dose for the 2/20 Gy and the 5/10Gy experimental data sets; two-way ANOVA with Dunnett's posttest: *P < 0.05, **P < 0.01, ***P < 0.001, ****P < 0.0001.